# Analytical and Numerical Treatment of Resistive Drift Instability in a Plasma Slab

V.V. Mirnov,[1, a)] J.P. Sauppe,[1] C.C. Hegna,[1] and C.R. Sovinec[1]
*University of Wisconsin - Madison and the Center for Magnetic Self-Organization in Laboratory and Astrophysical Plasmas, Madison, Wisconsin, USA*

An analytic approach combining the effect of equilibrium diamagnetic flows and the finite ion-sound gyroradius associated with electron-ion decoupling and kinetic Alfvén wave effects is derived to study resistive drift instabilities in a plasma slab. Linear numerical computations using the NIMROD code are performed with cold ions and hot electrons in a plasma slab with a doubly periodic box bounded by two perfectly conducting walls. A linearly unstable resistive drift mode is observed in computations with a growth rate that is consistent with the analytic dispersion relation derived here. The resistive drift mode is expected to be suppressed by magnetic shear in unbounded domains, but the mode is observed in numerical computations with and without magnetic shear. In the slab model, the finite slab thickness and the perfectly conducting boundary conditions are likely to account for the lack of suppression.

**Accepted for publication in:** *Plasma Physics Reports*



[a)] Electronic mail: vvmirnov@wisc.edu

## I. INTRODUCTION

Numerical modeling of two-fluid current-driven tearing modes in the presence of a pressure gradient[1] have revealed a fluctuation that is destabilized by diamagnetic effects even in the absence of magnetic shear. Linear computations using the NIMROD code are performed for plasma slab with cold ions and hot electrons in a doubly periodic box bounded by two perfectly conducting walls. Within this computational model, configurations with magnetic shear were shown to be unstable to current-driven drift-tearing instability. Our work was originally motivated by a desire to understand the behavior of the drift-tearing mode as it transitions from the collisional to semi-collisional regimes. Previous authors[2,3] studied this in a periodic domain, and we sought to understand the transition in a bounded domain with perfectly conducting walls while also including the effects of finite electron thermal conduction. In addition to the drift-tearing mode, when performing these simulations we observe another linearly unstable mode driven by the pressure-gradient, which we identify as a resistive drift mode.

The resistive drift instability, also known as the dissipative drift instability, was originally described in the potential approximation by S.S. Moiseev and R.Z. Sagdeev in Ref. 4. A comprehensive electromagnetic theory of this instability was presented by A.B. Mikhailovskii in his fundamental work.[5] In this paper, he performed a self-consistent analysis of the electron temperature perturbations and derived an elegant condition for validity of the electrostatic approximation. The electromagnetic fluid model was later extended by A.B. Mikhailovskii to kinetic calculations with the use of the model collisional operator.[6] It allowed the author to investigate the transition from rare to frequent collisions and obtain a unified picture of the drift-Alfvén instability at arbitrary collisionality. Following A.B. Mikhailovskii's works,[5,6] we present in this paper the analytical and computational results related to the electromagnetic resistive drift-Alfvén instability.

The inclusion of finite resistivity is a key element in numerical modeling of both drift-tearing and dissipative drift instabilities. In the drift wave case considered in the present paper, if the electrons are free to move along the magnetic field to cancel the charge separation, the Boltzmann distribution (adiabatic response) is provided, and the drift wave is stable. When the electron motion is delayed by electron-ion collisions, a phase shift appears that results in instability. The resistive drift instability occurs on temporal and spatial scales that differ from those inherent to the drift-tearing modes. This motivated our interest in the development of a model where both instabilities can be considered within the scope of one equilibrium configuration and dynamical framework.

An additional motivating factor emerges from the series of preceding papers.[2,3,7] In spite of the similarity of our equilibrium configurations, observations of the drift-type modes have not been reported in other linear computations.[2,3] However, in later nonlinear computations of the four-field model[7] two different saturated states were reported. The first has large islands typical of the usual saturated tearing instability, while the second has much smaller islands that rotate at roughly the electron diamagnetic frequency. The small island solutions have a character qualitatively consistent with electromagnetic drift waves which can be associated with the resistive drift-Alfvén modes. This was interpreted in Ref. 7 as a possible coupling between drift-tearing and drift waves, an opportunity pointed out earlier in Ref. 8.

There are two categories of non-MHD effects important for the physics of drift-tearing and resistive drift instability: (1) electron and ion diamagnetic flows caused by equilibrium pressure gradients, and (2) electron and ion decoupling on short scales associated with kinetic Alfvén waves (KAW). The second class accounts for parallel electron compressibility and becomes important at large ion-sound gyroradius $\rho_s$. The electron compressibility and relevant KAW physics of electron-ion decoupling were missed in earlier incompressible tearing calculations.[9] We have developed a unified analytical model which includes both of these effects and is universally valid for tearing and drift modes. It is a natural generalization of the previously studied force-free calculations[10] to the case of a non-uniform equilibrium pressure distribution. Our earlier analytical models[1] were derived either in the limit of infinitely large parallel electron heat conduction or in the pure adiabatic regime with an isentropic equilibrium. We report now a general analytical model with arbitrary equilibrium and finite parallel thermal conduction in Sec. III.A. The reduced version of this model with infinitely large electron thermal conduction is used in Sec. III.B to derive a resistive drift mode dispersion relation.

The results of our numerical computations with infinite electron thermal conduction are presented in Sec. IV. For configurations without magnetic shear, the analytical results are consistent with the numerical computations showing good accuracy and verifying NIMROD for the class of problems with small scale perturbations. In a sheared magnetic field, the resistive drift type instability is predicted to be suppressed by magnetic shear.[11,12] This conclusion applies to an infinite domain with mode propagation in the direction of the electron pressure gradient. Our computations are performed in a bounded domain, but the trend of decreasing growth rate with increasing shear is consistent with the analytical predictions. The analytical interpretation of the numerical results is discussed in the Summary.

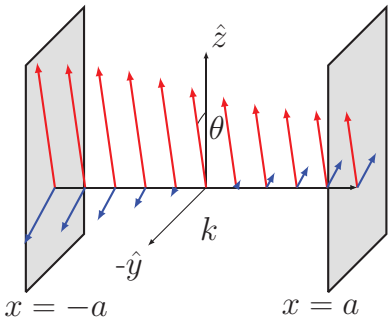


FIG. 1. The equilibrium magnetic configuration of the plasma slab with the sheared component $B_y^{(0)}/B_0 = f(x)$ where $f(x)$ is given by (3). It is converted to uniform field with $B_y^{(0)}/B_0 = \sin\theta$ at $\epsilon = 0$ or $L_s = \infty$ and to $B_y^{(0)}/B_0 = \epsilon \sin(x/L_s)$ at $\theta = 0$.

## II. EQUILIBRIUM CONFIGURATION

For our analytical and numerical calculations we consider a sheared slab equilibrium with straight magnetic field lines parallel to the $yz$-plane. Their mutual orientation varies with $x$. The corresponding equilibrium magnetic field is given by

$$\mathbf{B}^{(0)} = B_0(x)(\mathbf{e}_z\sqrt{1-f^2} + \mathbf{e}_y f), \qquad |\mathbf{B}^{(0)}| = B_0(x), \tag{1}$$

where $\mathbf{e}_y$ and $\mathbf{e}_z$ are the two mutually perpendicular unit vectors along the $y$ and $z$ axis. Non-uniform plasma pressure $p^{(0)}(x)$ is balanced by $x$-dependent amplitude $B_0(x)$ such that

$$B_0^2(x) = B_0^2(0) + 8\pi p^{(0)}(0) - 8\pi p^{(0)}(x). \tag{2}$$

The equilibrium magnetic field is a superposition of a guide field, $B_z^{(0)}$, and a relatively small sheared component, $B_y^{(0)}$. The strength of the sheared component is determined by the choice of $f(x)$:

$$f(x) = \sin\left[\theta + \arcsin\left(\epsilon \sin\left(\frac{x}{L_s}\right)\right)\right] \ll 1. \tag{3}$$

If $\theta = 0$, then $\epsilon \ll 1$ characterizes the strength of the sheared field relative to the guide field and $L_s$ is the shear scale length. The constant angle $\theta \ll 1$ determines the angle between $\mathbf{B}^{(0)}$ and $\mathbf{e}_z$ at $x = 0$ as shown in Fig. 1. It is introduced for flexibility in orienting the wave vector and the uniform magnetic field in case of shear-free configurations with $\epsilon = 0$ or $L_s = \infty$. The equilibrium field (1)-(3) is obtained by rotation of the standard doubly periodic configuration with the sheared component $\propto \sin(x/L_s)$ in angle $\theta$ over the $x$-axis.

The equilibrium current density consists of the parallel component and cross-field diamagnetic current

$$\mathbf{j}^{(0)} = \lambda\mathbf{B}^{(0)} + \frac{c}{B_0(x)}\frac{dp^{(0)}}{dx}(\mathbf{e}_y\sqrt{1-f^2} - f\mathbf{e}_z), \tag{4}$$

where $\lambda = cf'(x)/4\pi\sqrt{1-f^2}$. In the $x$-direction, the plasma slab is bounded by two perfectly conducting surfaces which are parallel to the $yz$-plane and placed at $x = \pm a$, as shown in Fig. 1. With the periodic structure of $f(x)$, the possibility of multiple resonances for tearing modes exists. To avoid these complications, we constrain the size of the box in the $x$-direction to satisfy $a < \pi L_s$. At $\theta = 0$, this ensures the existence of a single resonant location at $x = 0$ for perturbations uniform in the $z$ direction.

We consider a plasma equilibrium with cold ions and hot electrons. Numerical computations are performed for the equilibrium configurations with electron pressure gradient supported by non-uniform density at constant electron temperature. The general case of both non-uniform density and electron temperature is treated analytically. In all equilibrium states, the plasma is at rest, $\mathbf{v}^{(0)} = 0$, while the existence of the non-zero equilibrium electron velocity, $\mathbf{v}_e^{(0)} = \mathbf{j}^{(0)}/en^{(0)}$, leads to additional diamagnetic terms in the linearized plasma evolution equations.

## III. TWO-FLUID MHD MODEL

Both analytical and numerical treatments of the plasma dynamics are based on the plasma momentum balance equation

$$\rho\frac{d\mathbf{v}}{dt} = -\nabla\left(p + \frac{B^2}{8\pi}\right) + \frac{1}{4\pi}(\mathbf{B}\cdot\nabla)\mathbf{B}, \tag{5}$$

and generalized Ohm's law

$$\mathbf{E} + \frac{1}{c}\,\mathbf{v}\times\mathbf{B} = \frac{1}{nec}\,\mathbf{j}\times\mathbf{B} - \frac{\nabla p_e}{ne} - \frac{m_e}{e}\frac{d\mathbf{v}_e}{dt} + \eta\mathbf{j}, \tag{6}$$

which describes the balance of the electron momentum. In the analytical part of the work, viscous effects are ignored, $\nabla\cdot\pi_s = 0$, for both electrons and ions. A small ion viscosity is included in the NIMROD computations for numerical convenience. The effects of the thermal force contribution to the friction is ignored in both analytic and numerical calculations.

The electron inertia term is omitted in the analytical model; it is retained in the numerical computations and shown to be unimportant for the resistive drift instability in the parameter range considered in this paper. However, the effect of finite electron mass will certainly be significant for application of our model to weakly collisional or pure collisionless regimes of the drift-tearing instability. In the latter case, for example, the Hamiltonian form of the equations was shown to be effective for studying the diamagnetic effects on collisionless magnetic reconnection.[13]

The ion velocity $\mathbf{v}_i$ is associated with the fluid velocity $\mathbf{v}$ (center of mass velocity), $\mathbf{v}_i = \mathbf{v}$. To leading order in the ratio of electron to ion mass the electron velocity is expressed in terms of $\mathbf{v}$ and magnetic field $\mathbf{B}$ by making use of Ampere's law

$$\mathbf{v}_e = \mathbf{v} - \frac{c\nabla\times\mathbf{B}}{4\pi ne}. \tag{7}$$

The electron temperature equation includes parallel and diamagnetic heat fluxes

$$\begin{aligned}\frac{n}{\Gamma-1}\left(\frac{\partial T_e}{\partial t} + (\mathbf{v}_e\cdot\nabla)T_e\right) &= -p_e\nabla\cdot\mathbf{v}_e - \nabla\cdot\mathbf{q}_{\star e} + \nabla\cdot(\mathbf{b}\kappa_e(\mathbf{b}\cdot\nabla)T_e),\\ \mathbf{q}_{\star e} &= -\frac{\Gamma}{\Gamma-1}\frac{p_e c}{eB}\mathbf{b}\times\nabla T_e,\end{aligned} \tag{8}$$

where $\Gamma = 5/3, \mathbf{b} = \mathbf{B}/B$ and $\kappa_e = 3.16 p_e\tau_e/m_e$ is the parallel electron thermal conductivity. The latter is expressed in further calculations via the parallel electron thermal diffusivity $\chi_e = \kappa_e(\Gamma-1)/n$. The electron and ion continuity equations are identical and expressed by the plasma continuity equation

$$\frac{\partial n}{\partial t} \;+\; \nabla\cdot n\mathbf{v} = 0. \tag{9}$$

In order to close the equations we use Faraday's induction equation,

$$\frac{\partial\mathbf{B}}{\partial t} = -c\nabla\times\mathbf{E}, \tag{10}$$

and the plasma equation of state $p_e = nT_e$.

### A. Linearized Hall MHD Equations

Since the equilibrium configuration is uniform in the $y, z$-directions, we may decompose perturbations in terms of Fourier harmonics in these directions. Due to the flexibility in choosing the orientation angle $\theta$ in (3), the problem can be considered without loss of generality with the wave vector $\mathbf{k} = k\mathbf{e}_y$ oriented along $y$, so that $\partial/\partial z = 0$. Correspondingly, the equations (5)-(10) are linearized with respect to small perturbations of the form

$$\mathbf{B}(x,y,t) = \mathbf{B}^{(0)}(x) + \mathbf{B}(x)\;\exp(-i\omega t + iky), \tag{11}$$

$$\mathbf{v}(x,y,t) = \mathbf{v}(x)\exp(-i\omega t + iky). \tag{12}$$

Similar linearizations are applied to all other functions. In the linearized equations the zero-order quantities are labeled by the superscripts as in equation (12) while for simplicity of notation no superscripts are used for the first order corrections. With this choice of the wave vector, its parallel component with respect to the equilibrium magnetic field is determined by $B_y^{(0)}(x)$, $k_\parallel(x) = kB_y^{(0)}/B_0 = kf(x)$. If $\theta = 0$, then $k_\parallel(x) = \epsilon k \sin(x/L_s)$ with the resonant surface, $k_\parallel = 0$, located at $x = 0$. In the shear-free configuration with $\epsilon = 0$ or $L_s = \infty$, $k_\parallel = k \sin\theta$.

Following the derivation described in the Appendix results in two coupled equations for the first order quantities $B_x$ and $v_x$. The plasma momentum equation (5) yields the vorticity equation, or equivalently, the quasineutrality condition

$$\frac{\partial}{\partial x}\left(n^{(0)}\frac{\partial v_x}{\partial x}\right) - n^{(0)}k^2 v_x = -\frac{k}{4\pi\omega m_i}\left(B_y^{(0)}\nabla^2 B_x - B_x\frac{d^2 B_y^{(0)}}{dx^2}\right). \tag{13}$$

The induction equation (10) is used to derive the second relationship between these variables. It is obtained by considering the $x$-component of equation (10). Applying the curl operator to the electric field (6) eliminates the gradient of the electron pressure in the $x$-component. However, the important two-fluid effect associated with the parallel electron compressibility and electron-ion decoupling on short scales is recovered through the curl of the Hall term. The corresponding transformations lead to an expression proportional to the guide field perturbation $B_z$. The evolution of this quantity is based on the $z$-component of the equation (10). By making use of the explicit solution for $B_z$ (as detailed in the Appendix), the $x$-component of the induction equation is transformed to a form that establishes the second relationship between $B_x$ and $v_x$

$$(\omega B_x + k v_x B_y^{(0)})\left[1 - \left(\frac{\omega_{\star e}^{(n)}}{\omega} + \frac{\omega_{\star e}^{(T)}}{z_2}\right)\frac{\omega^2 z_2}{\omega^2 z_2 - k_\parallel^2 c_s^2 z_1}\right] = \frac{ic^2\eta}{4\pi}\nabla^2 B_x - \frac{\omega k_\parallel^2 c_s^2 d_i^2 z_1}{\omega^2 z_2 - k_\parallel^2 c_s^2 z_1}\left(\nabla^2 B_x - \frac{B_x}{B_y^{(0)}}\frac{d^2 B_y^{(0)}}{dx^2}\right), \tag{14}$$

$$z_1 = \Gamma\omega + ik_\parallel^2\chi_e, \qquad z_2 = \omega + ik_\parallel^2\chi_e, \qquad c_s^2 = \frac{T_e}{m_i}, \qquad d_i = \frac{c}{\omega_{pi}}.$$

This form represents a generalization of the force-free two-fluid tearing calculations[10] to the case of non-uniform plasma pressure.

The first term in the round brackets on the LHS of equation (14) expresses the combination describing the frozen-in condition in single-fluid ideal MHD. The terms in the square brackets originate from the equilibrium density and electron temperature gradients. They are presented by the two diamagnetic frequencies

$$\omega_{\star e}^{(n)} = -\frac{kcT_e^{(0)}}{eB_0 n^{(0)}}\frac{dn^{(0)}}{dx}, \qquad \omega_{\star e}^{(T)} = -\frac{kc}{eB_0}\frac{dT_e^{(0)}}{dx}. \tag{15}$$

The functions $z_1$ and $z_2$ describe the interplay between the adiabatic electron temperature response at $\chi_e = 0$ and the pure isothermal response that dominates in the limit $\chi_e \to \infty$. They provide a transition from the full pressure gradient driven diamagnetic frequency $\omega_{\star e}^{(p)} = \omega_{\star e}^{(n)} + \omega_{\star e}^{(T)}$ to the diamagnetic frequency $\omega_{\star e}^{(n)}$ determined by the density gradient. The functions $z_1$ and $z_2$ also control the speed (isothermal or adiabatic) of propagation of the slow magneto-acoustic waves (MA). Coupling with the slow magneto-acoustic waves is included in equation (14). When parallel ion motion is ignored, i.e. $c_s \to 0$ on the LHS of (14), the expression in the square brackets is consistent with the similar expression of Ref. 4.

The first term on the RHS of equation (14) represents the contribution from the plasma resistivity while the second term reflects the physics associated with the decoupling of electrons and ions on short scales and the transition to the kinetic Alfvén wave mediated regime of the tearing instability. Consider, for example, the case of a perfectly conducting, $\eta = 0$, uniform plasma and magnetic field. The solution of the vorticity equation (13) reads

$$v_x = -\frac{k_\parallel B^{(0)}}{4\pi\omega n^{(0)} m_i} B_x. \tag{16}$$

Substituting (16) in (14), ignoring electron thermal diffusivity, $\chi_e = 0$, and using the relationship $\nabla^2 B_x = -k_\perp^2 B_x$, yields the dispersion relation for the shear Alfvén and slow magneto-acoustic modes modified by the two-fluid effects. The corresponding modification of the Alfvénic branch has a form of the kinetic Alfvén wave dispersion relation

$$\omega^2 = k_\parallel^2 v_A^2 (1 + k_\perp^2 \rho_s^2). \tag{17}$$

where the adiabatic ion-sound gyroradius $\rho_s^2 = c_s^2\Gamma/\omega_{ci}^2$ (see Refs. 10 and 14).

In obtaining the explicit solution for $B_z$ from (A4), the term $c^2\eta\nabla^2 B_z/4\pi$ describing resistive diffusion of $B_z$ was neglected compared to the major contribution from plasma compressibility $B_z^{(0)}\nabla\cdot\mathbf{v}$ on the RHS of this equation. Combining equations (A5)-(A7) allows us to estimate the plasma compressibility and express it in terms of $B_z$ and $\nabla\cdot\mathbf{v} \simeq (-i\omega/\beta)(B_z/B_z^{(0)})$. Comparing this term with the $B_z$ resistive diffusion term in equation (A4) gives the condition when the latter effect can be ignored. This yields the condition of applicability of equation (14) in terms of an upper limit on $\beta$ or plasma resistivity

$$\beta \ll \frac{4\pi\omega\delta^2}{c^2\eta} \tag{18}$$

where $\delta$ is the characteristic scale of spatial variations of $B_z$.

In the case of the tearing modes, the explicit form of this inequality was, for example, analyzed in Ref. 10. In the case of the resistive drift modes, the operator $\nabla^2 B_z$ is converted into the algebraic relation $\nabla^2 B_z \simeq -k_\perp^2 B_z$. This simplifies the problem and allows us to obtain the explicit expression for $B_z$ from (A4) with the effect of the $B_z$ resistive diffusion taken into account. The corresponding straightforward transformations leads to the modified version of equation (14) which is valid for the resistive drift modes only. The structure of the modified equation is similar to (14) with some additional factors in $\omega$-dependent terms that are responsible for the resistive damping of the slow magnetoacoustic waves. The corresponding changes are illustrated by the analytical dispersion relation presented below which is valid now for the values of $\beta$ and plasma resistivity not limited by inequality (18).

### B. Analytical Dispersion Relation

Contrary to tearing mode theory, where the vorticity equation (13) is treated as a second order ODE, the fastest growing resistive drift mode is developed at $ka \gg 1$. Keeping the leading terms with $y$-derivatives in (13) yields the solution (16). Substituting (16) in (14) results in a second order ODE for $B_x(x)$ with the coefficients depending on $x$. For qualitative analytical treatment, the resulting equation is solved approximately by considering the $x$-dependent factors as constant. The solution satisfying zero boundary conditions at $x = \pm a$ has the form of a standing wave, $B_x = C\cos(n\pi x/2a)$ $(n = 2m+1)$. The dispersion relation is presented in the dimensionless form in the limit of infinitely large electron thermal diffusivity $\chi_e \to \infty$ (the case considered in numerical computations)

$$\left(\Omega - \frac{k_\parallel^2}{\Omega} + \frac{i\beta k_\perp^2}{S}\right)\left(1 - \frac{\Omega_{\star e}^{(n)}\Omega}{\Omega^2 - k_\parallel^2\beta + i\beta k_\perp^2\Omega/S}\right) - \frac{\Omega\beta k_\parallel^2 k_\perp^2 d_i^2}{\Omega^2 - k_\parallel^2\beta + i\beta k_\perp^2\Omega/S} + \frac{ik_\perp^2(1-\beta)}{S} = 0, \tag{19}$$

$$k_\perp^2 = k^2 + \frac{\pi^2 n^2}{4}, \qquad \Omega = \omega\tau_A, \qquad \Omega_{\star e}^{(n)} = \frac{\beta d_i k}{L_n}, \qquad S = \frac{\tau_R}{\tau_A},$$

where $L_n \to L_n/a$ is the dimensionless density gradient scale length while our definition of $\beta$ differs from the usual one by the factor 2

$$\beta = \frac{4\pi T_e^{(0)} n^{(0)}}{{B_z^{(0)}}^2}. \tag{20}$$

The dispersion relation is a fourth order polynomial for the complex frequency $\Omega$. In general, it has three stable and one unstable roots which are functions of the normalized wave numbers $k_\parallel \to k_\parallel a$ and $k_\perp \to k_\perp a$ and plasma parameters. According to Ref. 4, the limiting case of the electrostatic perturbations is equivalent to omitting the term proportional to $\Omega$ in the first round brackets in (19) ($\Omega \ll k_\parallel$). In the $S \to \infty$ limit, a simplified dispersion relation for the pure real frequency of the drift mode is derived and given by

$$(1 + k_\perp^2\rho_s^2)\Omega^2 - \Omega_{\star e}^{(n)}\Omega - k_\parallel^2\beta = 0 \tag{21}$$

with the isothermal ion-sound gyroradius $\rho_s^2 = d_i^2\beta$.

The $\rho_s$ factor originates from the third term in (19). In drift waves publications, it is associated with the ion polarization drift and influence of ion inertia (see, for example, Ref. 15). It is similar to the finite Larmor radius (FLR) stabilization effects. The FLR factor reduces the frequency and the growth rate of the unstable modes at large

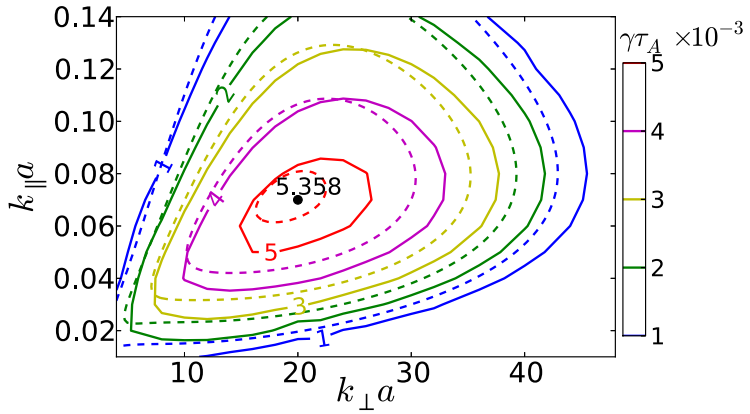


FIG. 2. Contour plot of the resistive drift mode growth rate $\gamma\tau_A \times 10^{-3}$ as function of $k_\parallel a$ and $k_\perp a$ at $\beta = 0.1,\ d_i/a = 0.1,\ L_n/a = 2,\ S = 10^4, P_m = 0.001$. Solution of the analytic dispersion relation (19)(dashed lines) plotted with the numerical results from NIMROD (solid lines).

$k\rho_s \gg 1$. Contrary to its stabilizing role for the electrostatic drift modes, the same term leads to the enhanced two-fluid tearing instability associated with the KAW mechanism in the tearing mode theory (see, for example, Ref. 10). The contributions from the third term in (19) are stabilizing here because they are related to the different modes of oscillation. The KAW mediated regime of two-fluid tearing instability is based on the destabilized modified shear Alfvén branch (17). For the electrostatic drift mode (21), this branch is decoupled. The resistive drift instability is driven by the destabilized modified slow magneto-acoustic branch. Indeed, applying equation (21) to the uniform plasma with $\Omega_{*e}^{(n)} = 0$ yields the frequency of the mode

$$\Omega^2 = \frac{k_\parallel^2 \beta}{1 + k_\perp^2 \rho_s^2}. \tag{22}$$

This dispersion is consistent with the solution for the two-fluid slow magnetoacoustic wave (see equation (27) in Ref. 10).

Note, that the fast magnetoacoustic mode is eliminated from consideration by making use of the decoupling condition (A5). This condition is valid for modes with low enough frequencies $\omega \ll kc_s$. Estimating the drift mode frequency $\Omega \sim \Omega_{*e}^{(n)} \simeq \beta d_i k/L_n$ leads to the inequality $\beta \ll (L_n/d_i)^2$ which is well satisfied in the conditions considered here. A more rigorous restriction, $\beta \ll 1$, is imposed on $\beta$ in the explicit solution of (A4) for $B_z$ when the LHS of this equation is ignored compared to the term $-B_z^{(0)} \nabla \cdot \mathbf{v} \simeq i\omega B_z/\beta$ on the RHS.

We now perform a parametric analysis of the analytical dispersion relation (19); the results are compared to the computational results in the Summary. The growth rate of the unstable mode $\gamma(k_\parallel, k_\perp)$ starts from zero at $k_\parallel = 0$ and reaches a sharp maximum as a function of $k_\parallel$ at small $k_\parallel \simeq 0.07$. The function $\gamma(k_\parallel, k)$ has a broad maximum as a function of $k$ at $k \simeq 30$ with the mode number in the $x$-direction $n_x = 1$. The maximum takes place at approximately $k\rho_s \simeq 1$ where the stabilizing FLR contribution becomes sizable. The contour plots of the dependence $\gamma(k_\parallel, k)$ obtained from the analytic dispersion relation (19) are illustrated by the dashed lines in Fig. 2 at $S = 10^4,\ \beta = 0.1,\ d_i = 0.1,\ L_n = 2$.

The real part of the unstable mode frequency is shown in Fig. 3. The dependence $\Omega_r(k_\parallel)$ follows the Alfvén wave dispersion $\Omega = k_\parallel$ at small $k_\parallel$. In this range, the mode character is predominantly electromagnetic. In the asymptotical limit of large $k_\parallel$, the dimensionless frequency grows with $k_\parallel$ slower than $k_\parallel$, $\Omega \to \sqrt{\beta} k_\parallel$, indicating that the perturbations are mainly electrostatic in this area. At the intermediate $k_\parallel$ related to the fastest growing mode, the deviation from the Alfvén wave dispersion is small. In this transient zone, the unstable mode is still substantially electromagnetic justifying the need of the full electromagnetic analysis at finite $\beta \simeq 0.1$.

To examine the scaling of the growth rate with the Lundquist number $S$, the dependence of $\gamma(k_\parallel, k)$ on $k_\parallel$ is obtained from the dispersion relation (19) and shown by the dashed lines in Fig. 4 at five different values of $S$, for fixed $k_\perp a$. As can be seen, the maximum of $\gamma$ monotonically increases with the decrease of $S$ in the range $10^5 \geq S \geq 5 \times 10^3$ showing the dominant role of resistivity in the mechanism of the mode growth. At $S = 10^3$, the growth rate decreases as the resistive damping of the slow magnetoacoustic mode exceeds the resistive drive for the dissipative drift instability. The interplay of these two factors determines the non-monotonic dependence of the growth rate on plasma resistivity.

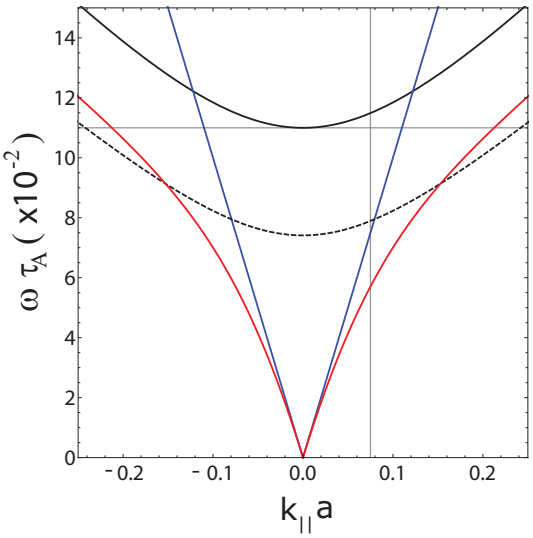


FIG. 3. Real part of the mode frequency $\omega\tau_A \times 10^{-2}$ vs $k_\parallel a$ from the dispersion relation (19) (red) and from the simplified equation (21) with FLR (dashed black) and w/o FLR (solid black curve shifted upward by $\Omega_{*e}^{(n)}$). Alfvén wave dispersion is shown by blue curves; the vertical and horizontal grid lines corresponds to $k_\parallel a$ of the fastest growing mode and $\Omega_{*e}^{(n)}$, respectively.

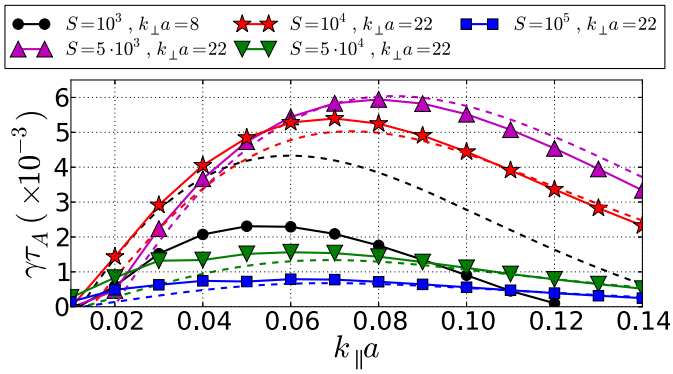


FIG. 4. Growth rate $\gamma\tau_A \times 10^{-3}$ dependence on $k_\parallel a$ for fixed values of $k_\perp a$ at five values of the Lundquist number $S$ and $\beta = 0.1$, $L_n/a = 2, d_i/a = 0.1$. Solution of the analytic dispersion relation (19)(dashed lines) plotted with the numerical results from NIMROD (solid lines).

## IV. NUMERICAL COMPUTATIONS

The NIMROD code[16,17] is used to solve Eqs. (5)-(6) in the slab configuration described in Sec. II. NIMROD is capable of including all of the terms in Eq. (8), but in the computations presented here, we take the electron response to be isothermal. As in Secs. II and III, the ions are taken to be cold.

The density profile is specified in the computations by the function

$$n^{(0)}(x) = n_0 \left[1 + \delta_n \tanh\left(x/\Delta_n\right)\right] \tag{23}$$

with $\delta_n = 0.1$ and $\Delta_n = 0.2a$. For this dependence, the inverse density length scale, $L_n^{-1} = (1/n)dn/dx$, is a function of $x$. At $x = 0$, our parameters give $aL_n^{-1} = 0.5$, which was also used for the previous analytical estimates in the paper.

NIMROD solves the extended MHD equations as an initial value problem. It may be run with only the linear effects or as a self-consistent nonlinear system; here, we run it in the linear regime. It has been benchmarked on plane-wave propagation in Ref. 17, on slab interchange without ion gyroviscosity in Ref. 19, and on slab ITG modes in the fluid limit in Ref. 18. While multiple modes may be unstable in the linear system, as an initial value code, NIMROD will

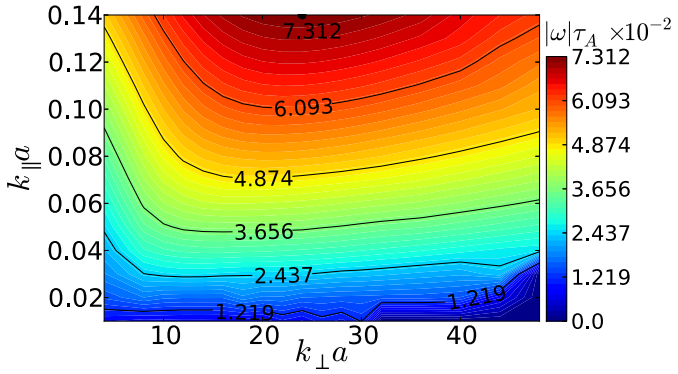


FIG. 5. Rotation frequency of the resistive drift mode as a function of $k_\parallel a$ and $k_\perp a$. ($\beta = 0.10$, $d_i/a = 0.1$, $S = 10^4$, $P_m = 10^{-3}$)

converge on the fastest growing mode. In cases with magnetic shear and large density gradients, both the drift-tearing mode and the resistive drift mode may be unstable.

Our computations without magnetic shear ($\epsilon = 0$) show an unstable resistive drift mode that grows preferentially with small $k_\parallel a$ and large $k_\perp a$, as illustrated by the solid lines in Fig. 2. With $\beta = 0.10$ and $d_i/a = 0.1$, the fastest growing mode has $k_\perp a = 20$ and $k_\parallel a = 0.07$. The fastest growth rate and the preferred orientation of the wavevector do not change monotonically with the two-fluid parameter, $\rho_s$. When $\beta$ is decreased from 0.10 to 0.05 at fixed $d_i/a = 0.10$, the maximum of the growth rate increases to $\gamma\tau_A = 6.829 \cdot 10^{-3}$, which occurs for $k_\perp a = 30$ and $k_\parallel a = 0.06$. When the ion skin depth is lowered from $d_i/a = 0.1$ to $d_i/a = 0.05$, (keeping $\beta = 0.05$) the maximum growth rate decreases to $\gamma\tau_A = 4.843 \cdot 10^{-3}$, at $k_\perp a = 36$ and $k_\parallel a = 0.07$.

The resistive drift mode frequency is typically an order of magnitude larger than the mode growth rate, and it varies strongly with $k_\parallel a$ and weakly with $k_\perp a$, as can be seen in Fig. 5. The frequency is monotonic with the two-fluid parameter, $\rho_s$; it decreases with both $\beta$ and $d_i/a$. However, the behavior of the frequency as a function of $k_\parallel a$ and $k_\perp a$ does not change substantially between these cases.

To examine the resistive drift mode's dependence on the plasma resistivity, computations with $\beta = 0.10$, and $d_i/a = 0.1$ are run at different values of $S$ and $k_\parallel a$, for fixed $k_\perp a$. For $S \geq 5 \times 10^3$, these scans are at $k_\perp a = 22$, roughly near the mode maximum in $k_\perp$ space, while for $S = 10^3$ the scan is performed at $k_\perp a = 8$ where the fastest growth rate is observed in this case. To mitigate the effects of the isotropic viscosity, it is held fixed between these computations; for $S = 10^5$, $P_m = 10^{-3}$, and smaller values of $S$ correspond to even smaller $P_m$.

The growth rate decreases as $S$ increases, as expected for a mode that depends on resistive effects, between $S = 5 \times 10^3$ and $S = 10^5$, as shown in the solid lines in Fig. 4. At $S = 10^3$, the growth rate again drops back down as the large resistivity begins to inhibit the growth of the mode. There is, overall, a favorable agreement between our computational results and the numerical solution shown in the dashed lines in Fig. 4 for the same parameters, although the analytic solution appears to be overestimating the growth rate at the lowest $S = 10^3$.

Previous work[11,12] has shown that the resistive drift mode is stabilized by magnetic shear in unbounded domains. We analyze the effects of a sheared magnetic field in our bounded domain computations with $\beta = 0.05$ and $d_i/a = 0.1$ by now varying the shear field strength, $\epsilon$, and the shear length, $aL_s^{-1}$. For each value of $\epsilon$ and $aL_s^{-1}$, we scan wavenumbers in the range $k_{\perp,0}a \in [0, 30]$ and $k_{\parallel,0}a \in [0, 0.06]$, where $k_{\perp,0}$ and $k_{\parallel,0}$ are the values at $x = 0$. This range includes the fastest growing pair ($k_\perp a = 30$, $k_\parallel a = 0.06$) when there is no magnetic shear. We find that the resistive drift mode is strongly stabilized by magnetic shear, as can be seen in Fig. 6. For modest values of shear strength, $\epsilon \lesssim 0.025$, the mode is quickly stabilized as the inverse shear length increases.

## V. SUMMARY

We present a unified two-fluid linear analytical model which includes electron and ion diamagnetic flows caused by equilibrium pressure gradients and electron and ion decoupling on short scales associated with the $\rho_s$ scale. It is a generalization of the force-free calculations[10] to the case of a non-uniform equilibrium distribution. The equilibrium profiles and the linear equations are universally valid for both uniform and sheared magnetic field configurations. The general case of arbitrary parallel electron thermal conduction is considered.

The term responsible for the electron-ion decoupling on short scales and associated with the ion-acoustic gyroradius, $\rho_s$, leads to two-fluid modification of the standard MHD branches of oscillations. The shear Alfvén mode is transformed

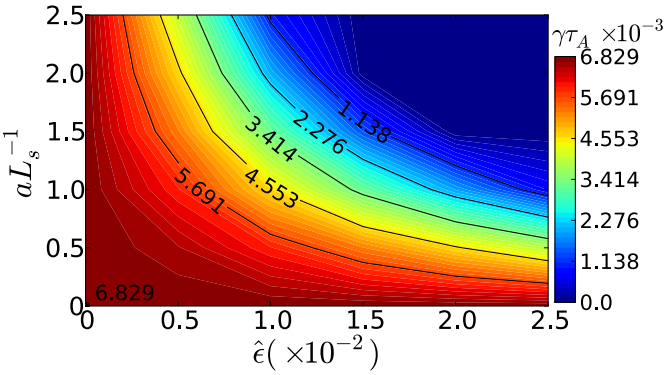


FIG. 6. Growth rates of the fastest growing resistive drift mode with $k_\perp a \in [0, 30]$ and $k_\parallel a \in [0, 0.06]$ as a function of the shear strength, $\epsilon$, and the shear length, $aL_s^{-1}$. ($\beta = 0.05$, $d_i/a = 0.1$, $S = 10^4$, $P_m = 10^{-3}$.)

to its fast kinetic Alfvén wave analog which is destabilized in tearing instabilities and in the electromagnetic regime of the resistive drift-Alfvén instability. The analog of the slow magneto-acoustic branch is further slowed by the so-called ion inertia or finite Larmor radius factor. This factor provides partial suppression of the growth rate in the electrostatic regime of the resistive drift instability.

A reduced version of the model with infinitely large electron thermal conduction is used to derive an approximate analytical dispersion relation for the resistive drift mode. Solutions for the mode growth rate show a strong dependence on $k_\parallel$ with a sharp maximum at small $k_\parallel \ll k$ and broad maximum as a function of $k_\perp a$ at large values $k_\perp a \sim 20 - 25$. This picture is consistent with the results of our numerical computations which also show a peak in the growth rate at small $k_\parallel$ with overall favorable matching of the analytical and numerical profiles considered as a function of two variables.

The scaling of the growth rate on the Lundquist number $S$ shows non-monotonic behavior. The growth rate increases as $S$ decreases in the range $S = 10^5$ and $S = 5 \times 10^3$. At $S = 10^3$, the computational results show sudden non-monotonic decrease of the growth rate. This is in agreement with the analytical results which predict a transition to the regime where resistive damping of the slow magnetoacoustic wave dominates the drive of the dissipative drift instability. Thus, for configurations without magnetic shear, the analytical results are consistent with the numerical computations showing good accuracy and verifying NIMROD for the problems with small scale perturbations.

Magnetic shear is predicted to suppress the resistive drift mode in unbounded domains, but it is observed in our bounded domain numerical computations even in the presence of shear. However, there is a strong decrease of the growth rate with both the shear strength, $\epsilon$, and the shear scale length, $aL_s^{-1}$, and the mode is stabilized for even modest values of one of these two parameters. Examining the data from our numerical computations, we empirically conclude that the effects of magnetic shear on the growth rate can be approximated as $\gamma\tau_A \sim \left(\epsilon a L_s^{-1}\right)^{-1}$.

## VI. ACKNOWLEDGMENTS

This material is based on work supported by the U.S. Department of Energy Office of Science, Office of Fusion Energy Sciences under Award Nos. DE-FG02-85ER53212, DE-FC02-05ER54814, and the U.S.NSF Cooperative Agreement PHY-0821899 Center for Magnetic Self-Organization in Laboratory and Astrophysical Plasmas.

### Appendix A: Linearized Hall MHD equations

Performing linearization of the generalized Ohm's law (6) with respect to the perturbations (12) yields the $x$-component of the induction equation (10)

$$\omega B_x = -k v_x B_y^{(0)} + \frac{ik^2 c B_y^{(0)}}{4\pi e n^{(0)}(x)} B_z - \frac{k j_y^{(0)}}{e n^{(0)}(x)} B_x + \frac{ic^2\eta}{4\pi}\nabla^2 B_x \tag{A1}$$

where Ampere's law is used to express $j_x$

$$j_x = \frac{ikc}{4\pi} B_z. \tag{A2}$$

Substituting (4) in (A1) and omitting small term proportional to $\lambda \propto \epsilon$ results in the equation for $B_x$ with the diamagnetic frequency $\omega_{\star e}^{(p)}$ in the Doppler shifted term

$$\begin{aligned}(\omega - \omega_{\star e}^{(p)}) B_x &= -k v_x B_y^{(0)} + \frac{ik^2 c B_y^{(0)}}{4\pi e n^{(0)}(x)} B_z + \frac{ic^2\eta}{4\pi}\nabla^2 B_x, \\ \omega_{\star e}^{(p)} &= -\frac{kc}{eB_0 n^{(0)}} \frac{d(n^{(0)} T_e^{(0)})}{dx}.\end{aligned} \tag{A3}$$

The $z$-component of the induction equation links $B_z$ with $B_x$ and plasma velocity components

$$\begin{aligned}-i\omega B_z =& - B_z^{(0)} \nabla\cdot\mathbf{v} + ikB_y^{(0)} v_z - v_x \frac{dB_z^{(0)}}{dx} - \frac{c}{4\pi e n_0(x)} \left( B_x \frac{d^2 B_y^{(0)}}{dx^2} - B_y^{(0)} \nabla^2 B_x \right) \\ &+ \frac{c^2\eta}{4\pi}\nabla^2 B_z + \frac{c}{e n_0^2(x)} \frac{dn^{(0)}}{dx} \left( \frac{1}{c}\mathbf{j}\times\mathbf{B}^{(0)} + \frac{1}{c}\mathbf{j}^{(0)}\times\mathbf{B} - \nabla p \right)_y .\end{aligned} \tag{A4}$$

The term proportional to $v_x$ can be omitted at $\beta \ll 1$. The resistive diffusion of $B_z$ is ignored assuming large enough $S \gg 2k_\perp L_n a/d_i \simeq 1.2\times 10^3$ (the numerical value is calculated in Sec. III). The last term in (A4) is put to zero to eliminate the fast magneto-acoustic mode. This is equivalent to the decoupling condition

$$B_z^{(0)} B_z = -4\pi p_e \to \frac{n}{n^{(0)}} = -\frac{1}{\beta}\frac{B_z}{B_z^{(0)}} - \frac{T_e}{T_e^{(0)}} \tag{A5}$$

where our definition of $\beta$ differs from the usual one by the factor 2

$$\beta = \frac{4\pi T_e^{(0)} n^{(0)}}{{B_z^{(0)}}^2}. \tag{A6}$$

The linearized plasma continuity equation reads

$$\nabla\cdot\mathbf{v} = i\omega\frac{n}{n^{(0)}} - \frac{v_x}{n^{(0)}}\frac{dn^{(0)}}{dx}. \tag{A7}$$

The $z$-component of the linearized momentum equation gives expression for $v_z$

$$v_z = -\frac{kB_y^{(0)}}{4\pi\omega n^{(0)} m_i} B_z + \frac{iB_x}{4\pi\omega n^{(0)} m_i}\frac{dB_z^{(0)}}{dx} \tag{A8}$$

Substituting (A7) and (A8) in (A4) and using ($A5$) gives equation for $B_z$ in terms of $B_x$, $v_x$, and $T_e$. The electron temperature perturbation is found from the linearized electron temperature equation (8)

$$\begin{aligned}-i(\omega - \omega_{\star e}^{(p)})\frac{T_e}{T_e^{(0)}} + \left( v_x - \frac{j_x}{en^{(0)}} \right)\frac{1}{T_e^{(0)}}\frac{dT_e^{(0)}}{dx} =& -(\Gamma-1)\nabla\cdot\mathbf{v}_e + i\chi_e k_\parallel \left( ik_\parallel \frac{T_e}{T_e^{(0)}} + \frac{B_x}{B_0}\frac{1}{T_e^{(0)}}\frac{dT_e^{(0)}}{dx} \right) \\ &+ i\Gamma\omega_{\star e}^{(p)}\frac{T_e}{T_e^{(0)}} - i\Gamma\omega_{\star e}^{(T)} \left( \frac{n}{n^{(0)}} + \frac{T_e}{T_e^{(0)}} - \frac{B_z}{B_z^{(0)}} \right)\end{aligned} \tag{A9}$$

where the equilibrium and perturbed electron velocities are given by (7) and (A2) while the electron compressibility is as follows

$$\nabla\cdot\mathbf{v}_e = i(\omega - \omega_{\star e}^{(p)})\frac{n}{n^{(0)}} + \left( \frac{ickB_z}{4\pi n^{(0)} e} - v_x \right)\frac{1}{n^{(0)}}\frac{dn^{(0)}}{dx}. \tag{A10}$$

The linearization of the parallel heat flux in (A9) is straightforward while the transformation of the $\mathbf{q}_{\star e}$ term involves the following steps

$$
\begin{aligned}
-\frac{\Gamma-1}{p_e^{(0)}}\nabla\cdot\mathbf{q}_{\star e} &= \frac{\Gamma c}{e p_e^{(0)}}\nabla\cdot\left[\frac{p_e\mathbf{B}}{B^2}\times\nabla T_e\right] = \frac{\Gamma c}{e n^{(0)}}\left(ik\frac{T_e}{T_e^{(0)}}\left[\nabla\times\frac{p_e^{(0)}\mathbf{B}^{(0)}}{B_0^2}\right]_y + \frac{1}{T_e^{(0)}}\frac{dT_e^{(0)}}{dx}\left[\nabla\times\frac{p_e\mathbf{B}}{B^2}\right]_x\right) \\
&= \frac{ikc\Gamma}{eB_0}\frac{dT_e^{(0)}}{dx}\left(\frac{p_e}{p_e^{(0)}}-\frac{B_z^{(1)}}{B_0}\right) - \frac{ikc\Gamma}{eB_0 n^{(0)}}\frac{dp_e^{(0)}}{dx}\frac{T_e}{T_e^{(0)}}.
\end{aligned}
\tag{A11}
$$

Making use of (A9) and relationships (A5), (A7) allows us to express algebraically the plasma compressibility $\nabla\cdot\mathbf{v}$ in terms of $v_x$, $B_x$ and $B_z$. Substituting this result in (A4), solving for $B_z$ and combining the solution with (A3) yields final equation (14) which is applicable for both drift-tearing and resistive drift modes.

The transformations involve a significant amount of straightforward algebraic manipulations. The derivation is essentially simplified by factoring into the combination $\omega B_x + k v_x B_y^{(0)}$ which appears on the LHS of the final equation (14) along with the expression in the square brackets. In performing the factoring, we followed the recipe suggested in Ref. 20 for the ordinary electromagnetic drift wave.

## References


[1] V.V. Mirnov, C.C. Hegna, J.P. Sauppe, and C.R. Sovinec, Bull. of the DPP APS 54th Annual Meeting, Oct. 29-Nov.2, Providence, RI, USA . **57**, 90 (2012).
[2] D. Grasso , M. Ottaviani , and F. Porcelli, Phys. of Plasmas **8**, 4306 (2001).
[3] D. Grasso , M. Ottaviani , and F. Porcelli, Nucl. Fusion **42**, 1067 (2002).
[4] S.S. Moiseev , and R.Z. Sagdeev, Zh. Tekh. Fiz **34**, 248 (1964).
[5] A.B. Mikhailovskii, Nucl. Fusion **12**, 55 (1972).
[6] A.B. Mikhailovskii, *Electromagnetic instabilities in an inhomogeneous plasma* (Institute of Physics Publishing, Bristol, Philadelphia and New York, 1992).
[7] M. Ottaviani, F. Porcelli, and D. Grasso, Phys. Rev. Lett. **93**, 075001 (2004).
[8] F. Waelbroeck, J. Connor, and H. Wilson, Phys. Rev. Lett. **87**, 215003 (2001).
[9] G. Ara, B. Basu, B. Coppi, G. Laval, M.N. Rosenbluth, and B.V. Waddel, Ann. Phys. (N.Y.) **112**, 443 (1978).
[10] V.V. Mirnov, C.C. Hegna, and S.C. Prager, Phys. of Plasmas **11**, 4468 (2004).
[11] P.K. Kaw , and P. Guzdar, *"Quadratic form for resistive-drift modes in a slab with magnetic shear", PPPL-1526, Princeton, NJ,* (1979).
[12] T.M. Antonsen, Phys. Rev. Lett, **41**, 33 (1979).
[13] E Tassi, F L Waelbroeck, and D Grasso, J. of Physics: Conference Series **260**, 012020 (2010).
[14] B.N. Kuvshinov, Plasma Phys. Control. Fusion **36**, 867 (1994).
[15] J. Weiland *Collective modes in inhomogeneous plasma* (Institute of Physics Publishing, Bristol and Philadelphia, 2000).
[16] C. R. Sovinec, A. H. Glasser, T. H. Gianakon, D. C. Barnes, R. A. Nebel, S. E. Kruger, D. D. Schnack, S. J. Plimpton, A. Tarditi, M. S. Chu, and the NIMROD Team, Journal of Computational Physics **195** 355-386 (2004).
[17] C. R. Sovinec, J. R. King, and the NIMROD Team, Journal of Computational Physics **229** 5803-5819 (2010).
[18] D. D. Schnack, J. Cheng, D. C. Barnes, and S. E. Parker, Physics of Plasmas (1994-present) **20** 062106 (2013).
[19] P. Zhu, D. D. Schnack, F. Ebrahimi, E. G. Zweibel, M. Suzuki, C. C. Hegna, and C. R. Sovinec, Phys. Rev. Lett. **101** 085005 (2008).
[20] R.J. Goldstone and P.H. Rutherford *Introduction to plasma physics* , New York, NY: Taylor & Francis Inc. (1995).